J Mater Sci (2011) 46:2338–2344
DOI 10.1007/s10853-010-5079-y

Characterization of CdTe nanocrystals during their synthesis in liquid paraffin: optical properties and particle growth

Georgi Yordanov · Hideyuki Yoshimura · Ceco Dushkin

Received: 4 October 2010 / Accepted: 10 November 2010 / Published online: 23 November 2010

Abstract This article presents a systematic investigation of the optical properties and the growth process of CdTe nanocrystals during their hot-injection-based synthesis in liquid paraffin. Cadmium(II) stearate and tributylphosphine telluride are used as precursors. The as-obtained nanocrystals are characterized by transmission electron microscopy (TEM) with energy dispersive spectroscopy (EDS), X-ray powder diffraction (XRD), UV–vis absorbance, and fluorescence spectroscopy. The changes in optical absorbance and fluorescence during the nanocrystal synthesis are studied. The average nanocrystal size and the mean nanocrystal concentration are derived from the optical spectra and their changes during the synthesis are investigated. It is found that synthesis at lower temperature (150 °C) favors the continuous nucleation and leads to the formation of relatively smaller nanocrystals (~3 nm in size), whereas the nanocrystal concentration is relatively constant during synthesis at higher temperature (250 °C) thus leading to the formation of larger nanocrystals (~5 nm in size).

Introduction

Semiconductor nanocrystals of size below 10 nm, known as quantum dots, exhibit a great potential as a new type of fluorophores for labeling and imaging of biological molecules due to their unique optical properties such as size-tunable fluorescence and narrow symmetric emission spectrum [1–7]. Cadmium telluride (CdTe) has been established as a suitable semiconductor material for the preparation of nanocrystals possessing tunable fluorescence in the visible spectrum with a high fluorescence quantum yield [8–12]. Chemical syntheses of CdTe nanocrystals are recently performed in aqueous medium [13–18], however, syntheses in organic solvents at high temperatures (the so-called hot-injection-based or hot-matrix syntheses) have also been developed [19–22]. The hot-injection-based methods usually provide a better control of the nanocrystal size and have been widely used for the production of monodisperse in size nanocrystals of CdX (X = chalcogenide) [23–28]. Therefore, any systematic investigation of the nanocrystal growth process and optical properties during hot-injection synthesis could provide a powerful tool for control of the nanocrystals size and optical characteristics. Moreover, it is important for deeper understanding of the intimate mechanisms of these processes, which are still rather unclear.

Previously, we have applied liquid paraffin as a solvent for the synthesis of high-quality nanocrystals of CdSe and CdS [29, 30]. We have used the synthesis in paraffin for a systematic investigation of the effect of temperature [31]. Various mixtures of stearic acid and liquid paraffin have been used as solvent systems for nucleation and growth of CdSe nanocrystals [32]. It has been found that many experimental parameters, such as the temperature, the precursors molar ratio, as well as the solvent system composition, could be used for fine control of the nanocrystals size and their optical properties.

The purpose of this article is to study the optical properties and the growth process of CdTe nanocrystals during their synthesis in liquid paraffin, which are not investigated

G. Yordanov (✉) · C. Dushkin
Faculty of Chemistry, University of Sofia, 1 "James Bourchier" Blvd, 1164 Sofia, Bulgaria
e-mail: g.g.yordanov@gmail.com

H. Yoshimura
Department of Physics, Meiji University, 1-1-1 Higashimita, Tama-ku, Kawasaki, Kanagava 214-8571, Japan

systematically so far. Cadmium(II) stearate and tributylphosphine telluride (TBP-Te) are used as precursors. The obtained nanocrystals are characterized by transmission electron microscopy (TEM) with energy dispersive spectroscopy (EDS), X-ray powder diffraction (XRD), UV–vis absorbance, and fluorescence spectroscopy. The changes in optical absorbance and fluorescence spectra during the nanocrystal synthesis are studied. The average particle size and the mean molar particle concentration can be calculated from the optical absorbance spectra as previously described [33]. Here, we apply this strategy to study the temporal evolution of the particle size and concentration during the nanocrystal growth at two different synthesis temperatures (150 and 250 °C).

Experimental section

Nanocrystal synthesis

The telluride precursor (tributylphosphine telluride, TBP-Te) is prepared under argon atmosphere by dissolving 410 mg (3.2 mmol) of tellurium powder (99.5%; Fluka) in 5 mL of tributylphosphine (TBP, 97%; Sigma) and 5 mL of liquid paraffin (RA.M.Oil S.p.A., Italy) for 90 min at 200 °C. Then, 20 mL of paraffin are added and the mixture is heated at 100 °C for 30 min (any unreacted tellurium is removed by filtration through a glass Schott-filter). The obtained clear yellow solution of TBP-Te is stored in a glass bottle under argon at room temperature. In each experiment, 50 mg (0.4 mmol) of CdO (Merck, Germany), 15 mL of liquid paraffin and 0.6 g (2.1 mmol) of stearic acid (Hatkim, Turkey) are put together in a reaction flask equipped with a reverse condenser, thermometer and mounted on a magnetic stirrer with a heating mantle. After heating at a temperature above 150 °C, the mixture becomes transparent (cadmium stearate is formed). Then 1.0 mL of the TBP-Te solution, equivalent to 0.25 mmol of tellurium, is fast injected in the flask at 150 or 250 °C. The reaction solution turns deep red, indicating for the formation and growth of CdTe nanocrystals. The temperature is kept constant throughout the entire synthesis. Three synthesizes are carried out at each temperature. Preliminary experiments showed that the growth rate and the nanocrystal size do not significantly depend on the stirring rate of the reaction solution.

Nanocrystal characterization

The nanocrystals are observed by a transmission electron microscope (TEM) JEM-2100F (JEOL) operated at 200 kV of acceleration voltage, equipped with a probe for energy dispersive spectroscopy (EDS). The nanocrystals are purified from unreacted precursors before TEM observation by a triplicate extraction with chloroform/methanol (1:1) mixture. X-Ray powder diffraction (XRD) patterns of purified nanocrystals are recorded at room temperature on a powder diffractometer Siemens D500 with CuKα radiation within 2θ range 20–70° and a step of 0.05° 2θ and counting time 2 s/step. Optical absorbance spectra of nanocrystal dispersions are measured by using a UV–vis spectrophotometer Jenway 6400. Quartz cuvettes are utilized for the measurements. All absorbance spectra are measured in toluene, containing TBP (1 vol.%) as a stabilizer. The fluorescence spectra of the samples are measured by a Carl Zeiss monochromator, equipped with a photo-multiplying tube (excitation of samples at 365 nm).

Monitoring the nanocrystal growth process

Changes in the nanocrystal size are traced by measuring the absorbance spectra of aliquots, collected from the reaction medium at given time intervals after mixing of precursors. About 0.1 mL of each aliquot is diluted in 2 mL of 1 vol.% TBP solution in toluene in order to prepare each sample for analysis by optical absorbance spectroscopy. The mass of each aliquot is accurately measured ($\pm$0.0001 g). Nanocrystal concentration can be determined from the absorbance spectra as previously described [33].

Results and discussion

The chemistry of nanocrystal formation

The hot-injection-based methods for synthesis of semiconductor nanocrystals basically include a fast injection of precursor into the reaction mixture at 280–320 °C; the formation of nanocrystals occurs within few seconds. The hot-injection syntheses of CdTe nanocrystals are phosphine-based, because they utilize trioctylphosphine telluride (TOP-Te) or the respective tributylphosphine derivative (TBP-Te) as precursors [23–29]. Cadmium(II) tetradecylphosphonate [25] could also be used as a Cd-precursor. It has been found that phosphonic salts of Cd(II) can be successfully replaced by Cd(II) carboxylates [27]. The chemical mechanism has been first discovered for the phosphine-based synthesis of PbX (X = S, Se, Te) nanocrystals [34]. Later research confirmed the same mechanism for the synthesis of Cd(II) chalcogenide nanocrystals [35]. It has been found that the chemical reaction between cadmium salts (carboxylates or alkylphosphonates) and tributylphosphine chalcogenide (TBP-X) leads to the formation of cadmium chalcogenide (CdX), tributylphosphine oxide (TBPO) and the respective acid anhydride. In our synthesis we combine Cd(II) stearate and TBP-Te as

precursors, dissolved in liquid paraffin as non-coordinating solvent. Figure 1 represents an illustration of the reaction scheme used to prepare the CdTe nanocrystals.

TEM and XRD studies

The preparation of CdTe nanocrystals, reported here, leads to the formation of spheroidal nanoparticles with a crystalline core and indistinct interface due to the capping layer. Figure 2 shows representative TEM images of CdTe nanocrystals prepared at different temperatures. High-resolution TEM images of single nanocrystals are shown as insets in Fig. 2, which clearly evidence the spheroidal shape and crystallinity of nanocrystals. Particles of size 3–5 nm are formed. This allows utilizing previously derived empirical formulae relating the average nanocrystal size of spheroidal particles with the position of exciton absorbance band [33]. Therefore, in the next discussions, we use the nanocrystal sizes calculated from the absorbance spectra. The EDS analysis shows the presence of Cd and Te in the nanocrystals. The presence of Cl results from residual chloroform, which is used as a solvent for the nanocrystals. EDS spectra taken from different areas of the sample show different Cd/Cl signal ratios. EDS spectra taken from an area, were the number of CdTe nanocrystals is larger, show higher Cd/Cl signal ratio. The XRD studies show that all diffraction peaks of CdTe nanocrystals (Fig. 3) belong to the cubic (zinc blende) structure. Three distinct diffraction peaks are observed at 2θ values of 23.7°, 40°, and 46.5° from the XRD spectrum, corresponding to the (111), (220), and (311) crystalline planes of cubic CdTe, respectively. The shoulder peaks to the left of the labeled (111) peaks in Fig. 3 are attributed to Cd(II) stearate. Our previous studies of the XRD pattern of Cd(II) stearate showed that its diffraction peaks appear at 2θ values of 22° and lower. [31]. The XRD pattern does not depend significantly on the preparation temperature (150 or 250 °C). The wide diffraction patterns result from the small nanocrystal size. Using the Scherrer formula one can calculate the approximate nanocrystal size from the XRD profiles, which is within the range 3–5 nm.

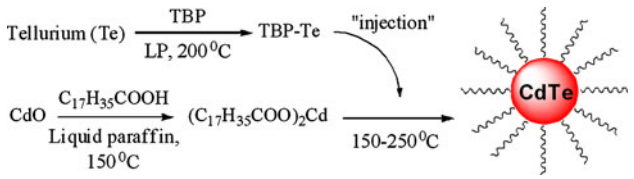

Fig. 1 Scheme of the preparation of stearate-coated CdTe nanocrystals

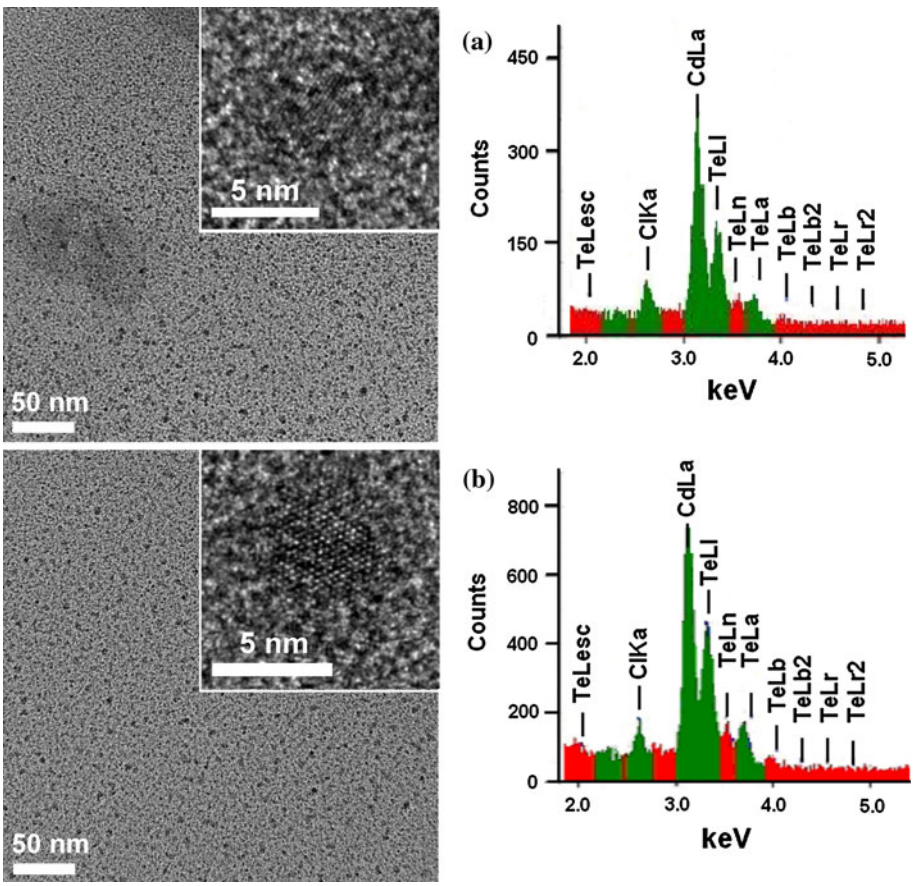

Fig. 2 TEM images (*left*) and the corresponding EDS-spectra (*right*) of CdTe nanocrystals, prepared in liquid paraffin hot-matrix at various synthesis temperatures: **a** 150 °C; **b** 250 °C. Time of growth in both cases is 5 min. *Size bars* on images represent 50 nm

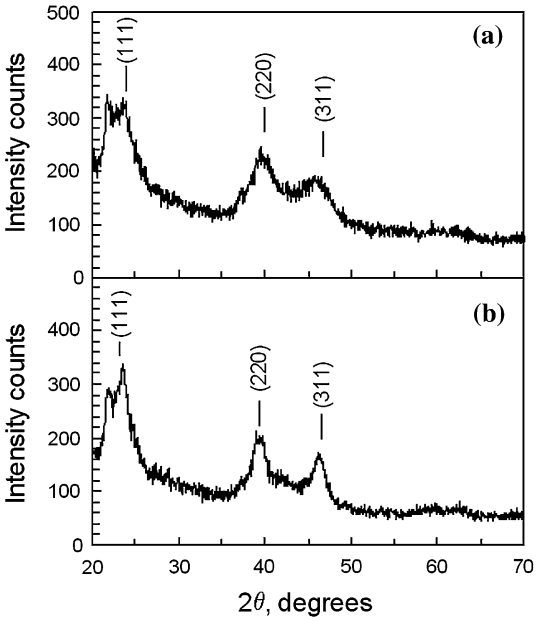

Fig. 3 XRD profiles of CdTe nanocrystals, prepared after 5 min of growth in liquid paraffin hot-matrix at: **a** 150 °C; **b** 250 °C

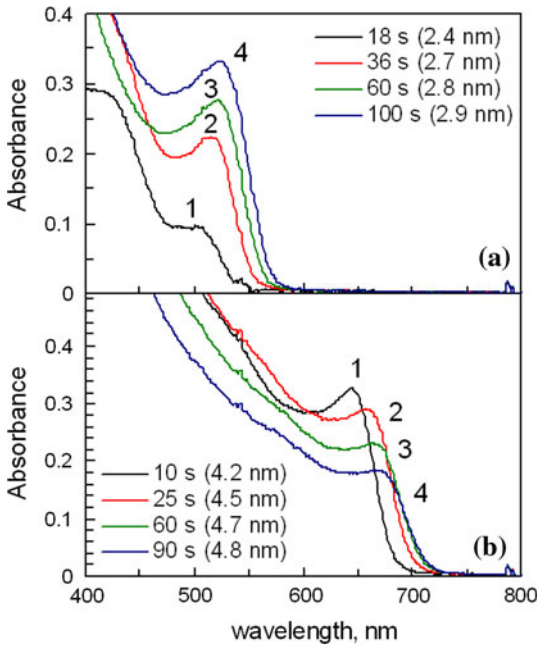

Fig. 4 Representative absorbance spectra of CdTe nanocrystals during growth at different synthesis temperatures: **a** 150 °C; **b** 250 °C. The spectra marked as (*1–4*) correspond to increasing the time of growth and the respective average nanocrystals diameter (as given in the legend)

Optical absorbance properties

The absorption transitions in the spectra of QDs at room temperature are not discrete, but absorption bands. The width of absorbance bands is a result of thermal (homogeneous) and inhomogeneous broadening, coming from the polydispersity of nanocrystal size [36]. Modern synthetic methods allow the production of relatively monodisperse in size nanocrystals of desired size and wavelength of optical absorbance [23–28]. As a result of the quantum confinement, the nanocrystal size reproducibly correlates with the wavelength of exciton absorbance maximum.

CdTe nanocrystals absorb light of wavelengths shorter than 820 nm that is determined by the band gap value (1.5 eV for bulk CdTe). As the particle size decreases, the band gap increases and the absorbance onset shifts to shorter wavelengths as a result from the effect of quantum confinement [37–40]. Therefore, the maximum of exciton absorbance is directly related to the nanocrystal size. The position of this maximum is used for calculation of the average nanocrystal diameter D (in nm) using the empirical formula [33]:

$$D = 9.8127 \times 10^{-7}\lambda^3 - 1.7147 \times 10^{-3}\lambda^2 + 1.0064\lambda - 194.84 \quad (1)$$

Here λ (in nm) is the wavelength at the maximum of the absorbance band.

Representative absorbance spectra of CdTe nanocrystals in the course of their synthesis are shown in Fig. 4. During the synthesis at 150 °C, the absorbance increases with time and the maximum shifts to longer wavelengths (Fig. 4a). The wavelength of maximum and the half-width at half-maximum (HWHM) of the exciton absorbance band of CdTe nanocrystals during their synthesis are given in Fig. 5. The red shift of absorbance corresponds to increase of the nanocrystal size during the synthesis. The slight increase of HWHM may result from increase of the width of the nanocrystal size distribution. Previous research demonstrated that HWHM could be used for qualitative evaluation of the nanocrystal size distribution (the wider size distribution results in larger value of HWHM) [36, 41].

During the synthesis at 250 °C, the absorbance decreases with time and the maximum shifts to longer wavelengths (Fig. 4b). The red shift indicates increase of the nanocrystal size during the synthesis (Fig. 5a). The decrease in absorbance as a function of reaction time observed in Fig. 4b could be a result of increasing the size distribution of nanocrystals. The HWHM of the absorbance spectra slightly increases (Fig. 5b), which could also be a result from increasing of the size distribution. Most probably, Ostwald ripening takes place at the high temperature during the nanocrystal growth in this case. All peculiar changes in the absorbance spectra of nanocrystals during their synthesis result from the complex nanocrystal growth process. Actually, the data from the absorbance spectra may be quite useful in realizing the nanocrystal growth during the synthesis as discussed further in "Nanocrystal nucleation and growth" section.

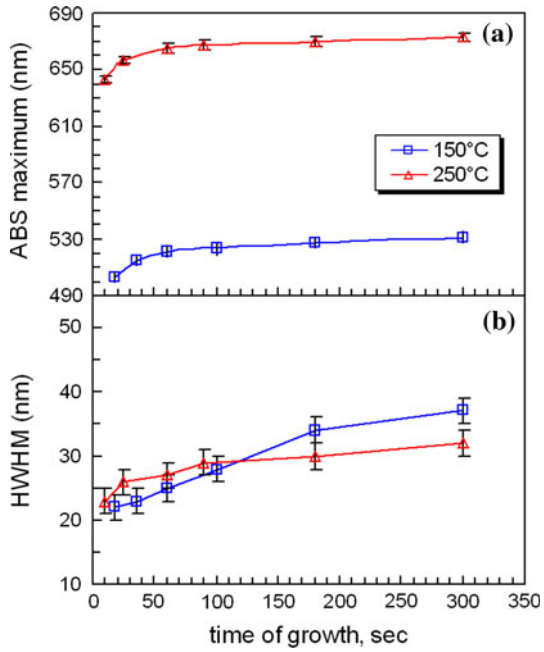

Fig. 5 Absorbance characteristics of CdTe nanocrystals during their growth in paraffin: **a** wavelength of the maximum of the exciton absorbance band, used for the calculation of nanocrystal size; **b** half-width at half-maximum (HWHM) of the exciton absorbance band

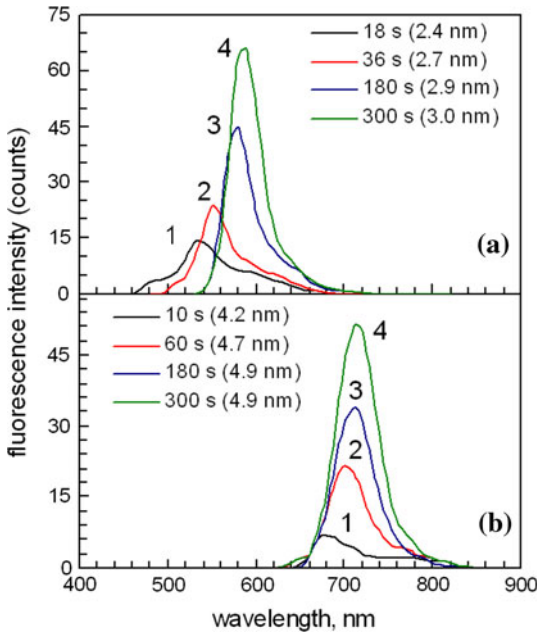

Fig. 6 Representative fluorescence spectra of CdTe nanocrystals during growth at different synthesis temperatures: **a** 150 °C; **b** 250 °C. The spectra marked as (*1–4*) correspond to increasing the time of growth and the respective average nanocrystals diameter (as given in the legend)

Fluorescence properties

The fluorescence spectra of nanocrystals are also size-dependent [42]. Nanocrystals usually exhibit two types of fluorescence: (i) band-edge fluorescence, resulting from decay of the excited electron into the ground state [43]; (ii) trap-state fluorescence, resulting from decay of a surface-trapped electron (an electron trapped in a defect on the nanocrystal surface) [43, 44]. The trap-state fluorescence has a low intensity or even it is absent for nanocrystals of high quality.

Representative fluorescence spectra of CdTe nanocrystals during their growth at different temperatures are shown in Fig. 6. The fluorescence maximum shifts to longer wavelengths as a result from the increase of nanocrystals size, similar to the red shift of the respective absorbance spectra [36–39]. In the early stages of nanocrystal formation, the fluorescence spectra consist of two overlapping emission bands—one broader (trap-state emission) and one narrower (band-edge emission). In later stages the trap-state emission almost disappears. This is probably a result from the decrease of surface states during the later stages of nanocrystal growth. Similar decrease of the trap-state emission intensity has been previously observed during the growth of CdSe nanocrystals at similar conditions [30–32]. Decrease of the full-width at half-maximum (FWHM) probably results from decrease of the broad trap-state emission component of the fluorescence spectrum

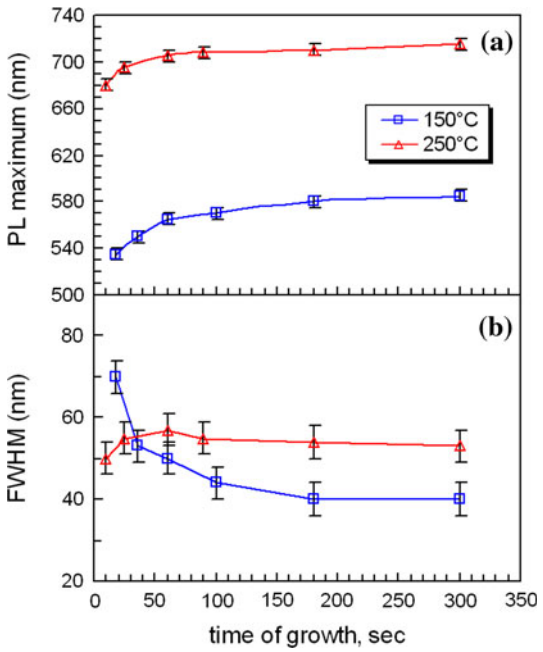

Fig. 7 Fluorescence characteristics of CdTe nanocrystals during their growth in paraffin: **a** wavelength of the maximum of the fluorescence (PL) band; **b** full-width at half-maximum (FWHM) of the fluorescence band

(Fig. 7b). The narrowing of the emission band in Fig. 7b could also be ascribed to a narrowing of the shape distribution of nanocrystals, although we have no direct evidence for this in our experiments.

Temporal evolution of the spectra (Fig. 6) shows a significant increase of the fluorescence intensity within the first 5 min during nanocrystal growth (longer reaction times do not lead to significant changes in the fluorescence intensity). This is the case for both syntheses at lower (150 °C) and higher (250 °C) temperature. Similar cases of increasing the fluorescence intensity within the first minutes of growth have been observed previously during the hot-matrix syntheses of CdSe nanocrystals in trioctylphosphine oxide (TOPO)-containing solvent systems [41, 45]. It is generally accepted that lower fluorescence intensity is probably due to the higher concentration of defects at the nanocrystal surface (e.g., unsaturated bonds, ion vacancies, or disorder), which gives rise to a higher density of mid-gap states acting as electron and hole traps. The initial period of nanocrystal synthesis after the hot-injection of precursor is characterized by rapid growth, which results in surface disorder, and thus low fluorescence intensity. Surface ordering and reconstruction can subsequently take place during annealing, thus reducing the concentration of defects and increasing the fluorescence intensity.

Nanocrystal nucleation and growth

The processes of nanocrystal formation and growth at the conditions of hot-matrix syntheses are rather complex [29–32, 46–54]. Compared to other types of nanocrystals, the colloidal semiconductors are more suitable for studying crystallization processes, because their strong size-depended optical properties can be utilized for this purpose [55]. The temporal evolution of UV–vis absorbance spectra has become a routine technique for monitoring the semiconductor nanocrystal growth process [46, 48]. This technique allows the calculation of nanocrystal size with a rather high accuracy of ±0.1 nm, as confirmed by high-resolution TEM measurements [33]. The in situ observation of nucleation and growth of CdSe nanocrystals has been found to be rather successful and informative [47]. The mean nanocrystal concentration can also be determined from the absorbance data. We use the formulae from [33] to derive the following equation:

$$[\mathrm{CdTe}] = \frac{A_\mathrm{m}(\mathrm{HWHM})}{180774 D^{2.12} l} \times \frac{V_\mathrm{s} 10^3}{m_\mathrm{al}} \quad (2)$$

Here, [CdTe] is the nanocrystal concentration (in mmol/kg), A_m the absorbance of sample (aliquot plus TBP-toluene solution) measured at the absorbance maximum (HWHM) is the half-width at half-maximum of the absorbance band measured at the longer wavelength side of exciton absorbance band (in nm), D the calculated nanocrystal diameter (in nm), l the length of optical cuvette (in cm), V_s the sample volume (in mL), and m_al the mass of aliquot (in grams). Previous estimations indicate that the values of calculated nanocrystal concentration have ±10–15% standard deviation [33].

The average nanocrystal diameter (D) and nanocrystal concentration, [CdTe], during the growth of CdTe nanocrystals at different synthesis temperatures are given in Fig. 8. Synthesis at 250 °C leads to the formation of nanocrystals of about 5 nm in diameter keeping constant particle concentration in the reaction medium (~20 μmol/kg). In this case the nucleation is very fast and takes place within the first few seconds, followed by growth of the resulting nuclei without continuous nucleation during the rest time of synthesis. This situation is similar to previously reported synthesis of CdSe nanocrystals in liquid paraffin at 265 °C [31]. This result is rather different from the synthesis at 150 °C. The obtained nanocrystals in this case are about 3 nm in diameter. The nanocrystal concentration in the reaction medium increases from 20 to 120 μmol/kg within a time period from 20 to 300 s after the injection of TBP-Te precursor. This is a result from the continuous nucleation of new particles during the synthesis. This is similar to the previously reported synthesis of CdSe nanocrystals in liquid paraffin at 180 °C [31]. One can conclude that the synthesis of nanocrystals at lower temperatures favors the continuous nucleation of larger number of particles leading to smaller final particle size. The nanocrystal concentration is relatively constant during the synthesis at higher temperatures thus leading to the formation of larger nanocrystals.

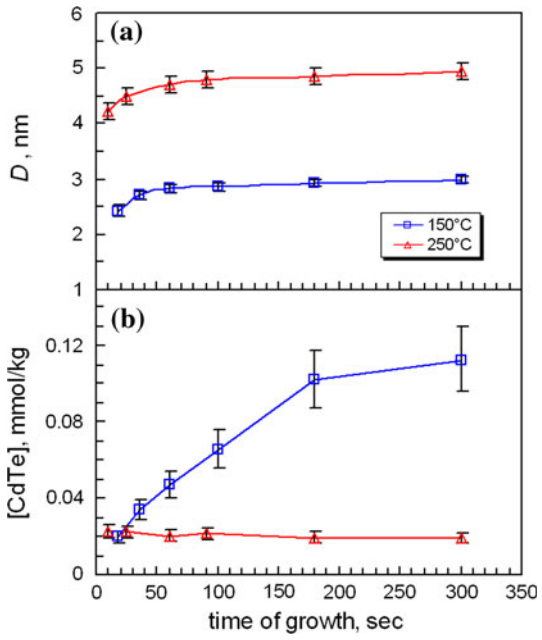

Fig. 8 **a** Average nanocrystal diameter (D) and **b** nanocrystal concentration, [CdTe], during synthesis at different temperatures (given in the legend)

Conclusions

It is found that the synthesis of CdTe nanocrystals from cadmium stearate and tributylphosphine telluride in liquid paraffin at temperatures 150–250 °C leads to the formation of dot-shaped nanocrystals of cubic (zinc blende) crystal structure. The UV–vis absorbance and fluorescence properties of nanocrystals are investigated during their synthesis. The average nanocrystal size and the mean nanocrystal concentrations are derived from the optical absorbance spectra and their changes during synthesis are studied. It is found that synthesis at lower temperature (150 °C) favors the continuous nucleation and leads to the formation of relatively smaller nanocrystals ($\sim$3 nm in size), whereas the nanocrystal concentration is relatively constant during the synthesis at higher temperature (250 °C) thus leading to the formation of larger nanocrystals ($\sim$5 nm in size). It is expected that the obtained results could be helpful for the synthesis of CdTe nanocrystals in the large scale, as well as for the deeper understanding of the mechanisms of nanocrystal formation and growth.

Acknowledgements This research was financially supported by the Bulgarian Ministry of Science and Education, Project DO 02-168.

References

1. Gao X, Yang L, Petros J, Marshall F, Simons J, Nie S (2005) Curr Opin Biotechnol 16(1):63
2. Sharma P, Brown S, Walter G, Santra S, Moudgil B (2006) Adv Colloid Interface Sci 123–126:471
3. Pinaud F, Michalet X, Bentolila L, Tsay J, Doosel S, Li J, Iyer G, Weiss S (2006) Biomaterials 27:1679
4. Zajac A, Song D, Qian W, Zhukov T (2007) Colloids Surf B 58:309
5. Jamieson T, Bakhshi R, Petrova D, Pocock R, Imani M, Seifalian A (2007) Biomaterials 28:4717
6. Smith A, Duan H, Mohs A, Nie S (2008) Adv Drug Deliv Rev 60:1226
7. Hild W, Breunig M, Goepferich A (2008) Eur J Pharm Biopharm 68:153
8. Dong W, Guo L, Wang M, Xu S (2009) J Lumin 129:926
9. Liu Y, Yu J (2009) J Colloid Interface Sci 333:690
10. Liu J, Liang J, Han H, Sheng Z (2009) Mater Lett 63:2224
11. Li L, Qian H, Fang N, Ren J (2006) J Lumin 116:59
12. Dubavik A, Lesnyak V, Thiessen W, Gaponik N, Wolff T, Eychmuller A (2009) J Phys Chem C 113(12):4748
13. Rogach A, Franzl T, Klar T, Feldmann J, Gaponik N, Lesnyak V, Shavel A, Eychmuller A, Rakovich Y, Donegan J (2007) J Phys Chem C 111:14628
14. Yang W, Li W, Dou H, Sun K (2008) Mater Lett 62:2564
15. Weng J, Song X, Li L, Qian H, Chen K, Xu X, Cao C, Ren J (2006) Talanta 70:397
16. Zhang Y, Zhang H, Ma M, Guo X, Wang H (2009) Appl Surf Sci 255:4747
17. Hu L, Mao Z, Gao C (2009) Colloids Surf A 336:115
18. Abd El-sadek M, Kumar J, Babu S (2010) Curr Appl Phys 10:317
19. Talapin D, Rogach A, Mekis I, Haubold S, Kornowski A, Haase M, Weller H (2002) Colloids Surf A 202:145
20. Kumar S, Nann T (2003) Chem Commun 19:2478
21. Xing B, Li W, Sun K (2008) Mater Lett 62:3178
22. Liu X, Jiang Y, Wanga C, Li S, Lan X, Chen Y, Zhong H (2010) J Cryst Growth 312:2656
23. Murray C, Norris D, Bawendi M (1993) J Am Chem Soc 115: 8706
24. Talapin D, Haubold S, Rogach A, Kornowski A, Haase M, Weller H (2001) J Phys Chem B 105(12):2260
25. Peng Z, Peng X (2001) J Am Chem Soc 123:183
26. Qu L, Peng A, Peng X (2001) Nano Lett 1(6):333
27. Yu W, Peng X (2002) Angew Chem Int Ed 41:2368
28. Yu W, Wang A, Peng X (2003) Chem Mater 15:4300
29. Yordanov G, Dushkin C, Gicheva G, Bochev B, Adachi E (2005) Colloid Polym Sci 284:229
30. Yordanov G, Gicheva G, Bochev B, Dushkin C, Adachi E (2006) Colloids Surf A 273:10
31. Yordanov G, Dushkin C, Adachi E (2008) Colloids Surf A 316:37
32. Yordanov G, Yoshimura H, Dushkin C (2008) Colloids Surf A 322:177
33. Yu W, Qu L, Guo W, Peng X (2003) Chem Mater 15:2854
34. Steckel J, Yen B, Oertel D, Bawendi M (2006) J Am Chem Soc 128:13032
35. Liu H, Owen J, Alivisatos A (2007) J Am Chem Soc 129:305
36. Alivisatos A, Harris A, Levinos N, Steigerwald M, Brus L (1988) J Chem Phys 89(7):4001
37. Rossetti R, Nakahara S, Brus L (1983) J Chem Phys 79(2):1086
38. Brus L (1984) J Chem Phys 80(9):4403
39. Rossetti R, Ellison J, Gibson J, Brus L (1984) J Chem Phys 80(9):4464
40. Yoffe A (1993) Adv Phys 42(2):173
41. Qu L, Peng X (2002) J Am Chem Soc 124(9):2049
42. Nirmal M, Brus L (1999) Acc Chem Res 32:407
43. Ramsden J, Webber S, Gratzel M (1985) J Phys Chem 89:2140
44. Hässelbarth A, Eychmüller A, Weller H (1993) Chem Phys Lett 203:271
45. Donega C, Hickey S, Wuister S, Vanmaekelbergh D, Meijerink A (2003) J Phys Chem B 107:489
46. Peng X, Wickham J, Alivisatos A (1998) J Am Chem Soc 120: 5343
47. Qu L, Yu W, Peng X (2004) Nano Lett 4(3):465
48. Peng Z, Peng X (2001) J Am Chem Soc 123:1389
49. Peng Z, Peng X (2002) J Am Chem Soc 124:3343
50. Bullen C, Mulvaney P (2004) Nano Lett 4(12):2303
51. Van Embden J, Mulvaney P (2005) Langmuir 21:10226
52. Bullen C, Van Embden J, Jasieniak J, Cosgriff J, Mulder R, Rizzardo E, Gu M, Raston C (2010) Chem Mater 22(14):4135
53. Wang L, Sun X, Liu W, Liu B (2010) Mater Chem Phys 120(1): 54
54. Wang L, Sun X, Liu W, Yu X (2010) Colloids Surf A 353(2–3):232
55. Vossmeyer T, Katsikas L, Gienig M, Popovic I, Diesner K, Chemseddine A, Eychmiiller A, Weller H (1994) J Phys Chem 98:7665